

# Electromagnetic Time Reversal for Online Partial Discharge Location in Power Cables: Influence of Signal Disturbance and Interfering Reflections from Grid Components

Antonella Ragusa<sup>1,2</sup>, Peter A. A. F. Wouters<sup>3</sup>, Hugh Sasse<sup>4</sup>, Alistair Duffy<sup>4,2\*</sup>, Farhad Rachidi<sup>5</sup>, Marcos Rubinstein<sup>6</sup>

<sup>1</sup>Faculty of Computing, Engineering and Media, De Montfort University, The Gateway, Leicester, LE1 9BH, UK

<sup>2</sup>The Institute of Marine Engineering, Italian National Research Council, via di Vallerano 139, 00128 Roma, Italy

<sup>3</sup>Department of Electrical Engineering, Eindhoven University of Technology, 5600 MB Eindhoven, The Netherlands

<sup>4</sup>Faculty of Computing Engineering and Media, De Montfort University, The Gateway, Leicester, LE1 9BH, UK

<sup>5</sup>School of Engineering, The École Polytechnique Fédérale de Lausanne, ELL 138 (Bâtiment ELL), Station 11, CH-1015 Lausanne, Switzerland

<sup>6</sup>Institute for Information and Communication Technologies, University of Applied Sciences and Arts Western Switzerland, 1401 Yverdon-les-Bains, Switzerland

\*apd@dmu.ac.uk

**Abstract:** In online single-sided partial discharge (PD) location, the measured PD reflection patterns are affected by the characteristics of all the components of the associated power network. This paper analyses the performance of a PD location method based on electromagnetic time reversal (EMTR) theory, when interfering reflections contribute to the transient signals emitted by the PD event. The topology analysed is a ring main unit (RMU) in a medium voltage (MV) grid with mixed cross-linked polyethylene (XLPE) and paper-insulated lead-covered (PILC) cable sections. The PD reflection patterns, observed at the RMU, are disturbed by the reflections coming from the impedance discontinuities of the circuit and by the reflections coming from the cable ends of the PILC cables connected to the RMU. The simulated configuration is chosen such that classical location techniques based on identifying individual reflection peaks from which the PD origin can be determined via differences in time of arrival tend to fail due to overlapping peaks and other signal distortion. The numerical investigation shows that the accuracy of the EMTR-based location method is robust against these effects.

## 1. Introduction

The localisation of partial discharge (PD) sources in the insulation material of power cables is one of the most suitable methods to monitor the grid integrity, avoiding faults and improving the reliability [1]. Online PD location is mostly performed using reflectometry or traveling wave techniques, such as those proposed in [2]-[5]. These techniques are based on the fact that a PD produces electromagnetic current and voltage pulses that travel towards the cable ends. In the online single-sided PD location method [2,3], a measurement system, at one cable end, detects the pulse coming directly from the PD source and the pulse reflected from the other cable end. The delay between their peaks allows to estimate the location of the PD source. In double-end [3] and multiple-end [4] location methods, synchronised measurements of the direct PD signals are performed in double or multiple points of the line, and the PD source is localised by the delay of these measurements.

In medium voltage (MV) grids, PD measurement units are installed inside a ring main unit (RMU) as shown in Figure 1 [6]. Typically, an RMU has one to five MV cables connected to it and an MV/low voltage (LV) distribution transformer. The observation point (OP) inside the RMU monitors one or more cable section between two RMUs [6]. The effectiveness of the online PD localisation is affected by several issues related to the noise level in an operating grid and the distortion of the PD signals during their propagation

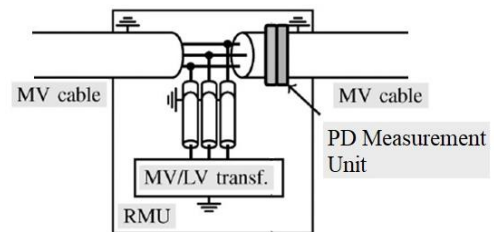


*Fig. 1 RMU with the PD measurement unit [6].*

along the line. This makes a proper identification of the PD signal peaks difficult [1]. A big challenge in single-sided PD localisation, monitoring a cable in an RMU, comes from the presence of the PD pulses reflected from other cables connected to the same RMU and from the connections at the other far end of the monitored cable. The distribution transformer in the RMU and the cable connecting the transformer to the busbar act as a complex impedance that often allows transmission from the other RMU connected cables. The PD return signals affect the measured PD signals at the OP making it difficult to locate the source with traditional methods like signal threshold discrimination.

In previous work [7]-[9], the authors have shown how PD localisation based on electromagnetic time reversal (EMTR) [10] overcomes the issues related to noise and distortion [8,9], using only one OP [7]. In [11], the authors

have shown that an EMTR-based method is a promising solution to address the issue related to the presence of the PD return signals, proposing a first numerical analysis of its effectiveness in a simple system formed by a cable monitored by an OP to which a second cable is connected. In this paper, a mixed cable circuit formed by cross-linked polyethylene (XLPE) and a paper-insulated lead-covered (PILC) three-phase cable section connected to an RMU is analysed. The XLPE section is also connected, at the other end, to a second PILC cables section. The PD events on the XLPE section are monitored by a measurement unit in the RMU. A detailed model of the complex impedance of the cables and of the RMU is used to reproduce the distortion of the PD signals due to the grid components.

The paper is organised as follows. In Section 2, the method based on the EMTR theory is briefly introduced. In Section III, the adopted models to reproduce the PD signal distortion and the PD reflection pattern due to the grid components, and of the complex impedance of cables and the RMU, is described. Finally, in Section 4 the performance of the EMTR method is analysed. The paper ends with conclusions presented in Section 5.

## 2. Time reversal method for PD localisation

The EMTR-based method for the PD localisation [7] is based on the invariance under time reversal of the Telegrapher's equations [10], describing the PD signal propagation on power lines, and on the use of the Transmission Line Matrix (TLM) numerical method [12] to solve the Telegrapher's equations in the time reversal domain. A detailed description of the method is reported in [7].

The basic steps of the EMTR-based PD localisation procedure are the following:

1. Measure the PD signal at one observation point (OP) along the power network.
2. Time-reverse the measured PD signal.
3. Define guessed PD locations (GPDs) in nodes of a 1D TLM model of the network.
4. Simulate the back-injection of the time-reversed PD signal for the different GPDs using the TLM method.
5. Localise the PD source by identifying the GPD characterized by the maximum energy.

The GPD node reproduces the line transverse impedance of the cable modified by the PD event [7]. The TLM numerical method is adopted to describe the time reversal propagation of the PD signals. The EMTR simulations are performed using a lossless 1D TLM model of the system under study. It has been demonstrated that a 1D TLM lossless model is sufficient to provide accurate results for measurements taken from a lossy cable [8]. In the 1D TLM model, the line is discretized into a series of  $N$  segments of length  $\Delta x$  as shown in Figure 2 (a). Each  $LC$  section is represented by a transmission line with a

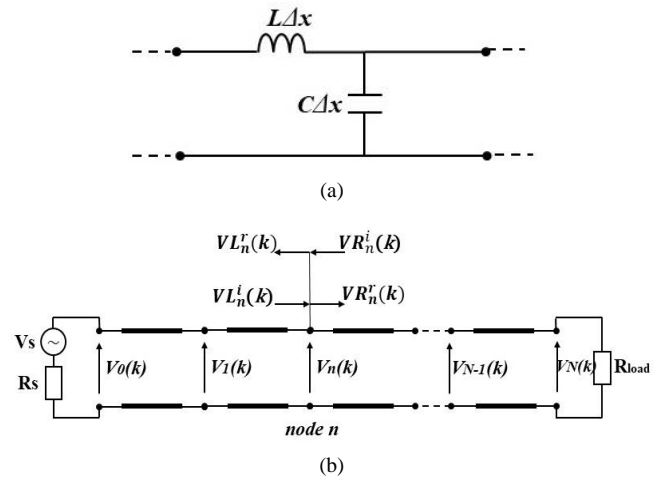


**Fig. 2** Equivalent circuit of a power line node (a) and its 1D TLM model (b) [12].

propagation speed,  $u$ , a characteristic impedance  $Z_c$ , and a transit time,  $\Delta t$ , given by equations (1) and (2):

$$u = \frac{1}{\sqrt{LC}} ; \quad Z_c = \sqrt{L/C} \quad (1)$$

$$\Delta t = \frac{\Delta x}{u} = \Delta x \cdot \sqrt{LC} \quad (2)$$

where  $L$  and  $C$  are, respectively, the per-unit-length longitudinal inductance and transverse capacitance of the line. The 1D TLM equivalent model of the line, obtained connecting the  $N$  sections, is shown in Figure 2 (b).

For each TR simulation, the energy  $E_n$  stored in the GPD transverse impedance is evaluated and normalized with respect to the maximum energy:

$$E_n = \frac{\frac{1}{2} C_{PD} \sum_{k=1}^M V_{GPD}^2(k)}{\frac{1}{2} C_{PD} \sum_{k=1}^M V_{GPDm}^2(k)} \quad \text{with} \quad M = \frac{T}{\Delta t} \quad (3)$$

where  $V_{GPDm}(k)$  is the maximum voltage over all the GPDs,  $C_{PD}$  is the GPD transverse capacitance modified by the PD event [7] and  $M$  the number of the samples. In this work, the first step, which is the experimental measurement of the PD signal in the real network, is substituted by a direct time (DT) simulation of the PD signal propagation in the system under study using a lossy model of the system that is able to reproduce the distortion of the PD signal during the propagation in a real system. It uses real cable design parameters and the modelling of the RMU response is based on measurements at several RMUs [13]. The used lossy model is described in the following section.

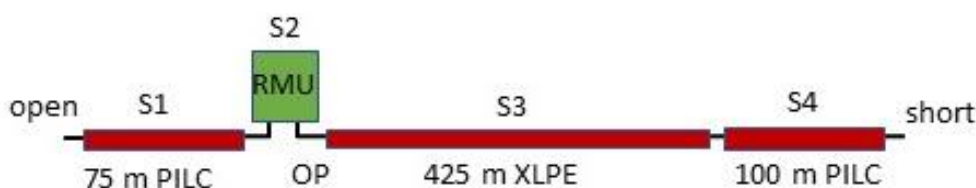


**Fig. 3** Configuration of the investigated cable configuration including an RMU.

### 3. Models of RMU and power cables

The adopted test configuration is the mixed cable circuit shown in Figure 3. The observation point (OP) is located at the XLPE connection at the RMU. The cable under test is an XLPE cable with length of 425 m connected at its end to a 100-m long PILC cable shorted at the second end. On the other side of the RMU there is a 75-m long PILC cable, opened at the other end. Short cable sections in grids can arise, e.g., after repairing a failed connection by replacing the defective part.

The inserted cable may have different signal propagation characteristics. The short and open ends represent a worst-case situation guaranteeing high reflection coefficients. The relatively short PILC cables at the ends cause multiple reflections, arriving shortly after each other. They obscure an easy identification of individual peaks. The waveform is further distorted by the presence of an RMU at the OP position. As detection takes place over all three phases, the three-phase cables will be modelled as single-conductor cables. Essentially, the topology has been designed to be a challenging test for the proposed method.

In tables 1 and 2 the characteristics of the XLPE and PILC cables are reported. The modelled cable characteristic impedances, velocities and attenuation coefficients are shown in Figure 4. In Figure 5, the simulated real and imaginary propagation coefficients (1-2-5 sequence from 1 kHz to 100 MHz) are plotted together with interpolated values (dots), needed for applying the inverse Fourier transforms.

The impedance at the cable ends can be frequency dependent, e.g., the input impedance of a consecutive cable or from components in an RMU. The characteristic cable impedance is approximated with a real value, taken as the average of the simulated absolute values between 100 kHz and 10 MHz (these values concern all phases in parallel with respect to the earth screen). The modelled frequency responses are shown in Figure 6 for both the current response and the voltage response. The main content is below 10 MHz and for the PD peak structure the frequency content below 100 kHz is less important. Whether the current or voltage component is measured depends on the type of detector used.

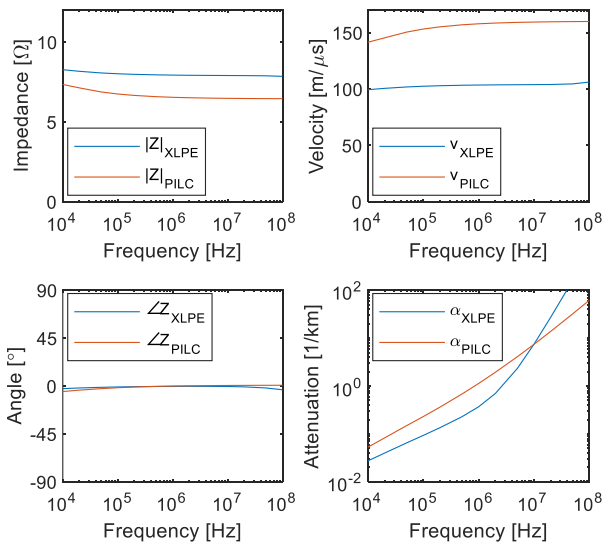


**Fig. 4** Characteristic impedance, velocity and attenuation for XLPE (blue) and PILC (red) cables.

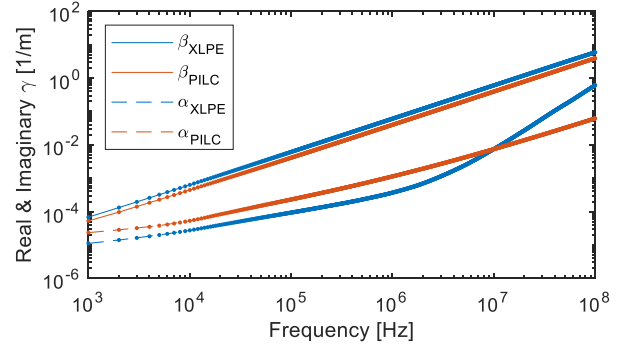
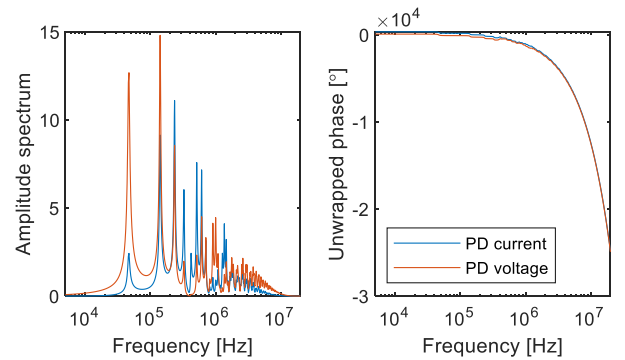


**Fig. 5** Real and imaginary part of the propagation coefficient for XLPE (blue) and PILC (red) cables; the dots indicate the resampling with frequency steps of 1 kHz.

In this paper, it is assumed that the signals are detected by means of a high frequency current transformer (HFCT), meaning that it is the PD current that is of interest.

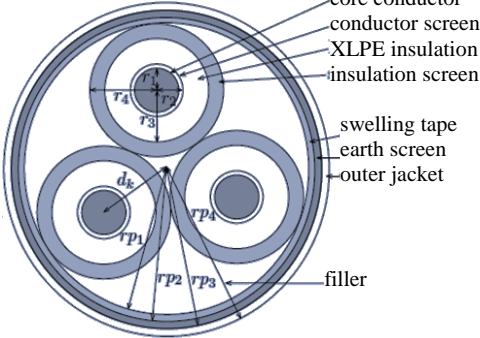
The RMU is modelled using the lumped component model shown in Figure 7 and proposed in [13]. Small RMUs are a few meters in size and are modelled as subdivided compartments, each containing a single network component. Usually, they contain one or a few MV cables connected to a busbar and a distribution transformer that feeds a local low-voltage grid. In Figure 7, compartments 1 and 2 contain the cables. Each of them is modelled as a transmission line with its characteristic impedance,  $Z_{c,1}$  and  $Z_{c,2}$  respectively of the XLPE and PILC cable. Inductances  $L_c$  and  $L_{bb}$ , related to loops from the connection to the busbar, are also considered. Compartment 3 contains the distribution transformer that behaves mainly capacitively at the main frequency components of a PD signal. It is modelled as a capacitance in series with an inductance and a resistance that are, respectively,  $C_{tr}$ ,  $L_{tr}$ ,  $R_{tr}$ . Finally,  $C_{icc}$ ,  $L_{icc}$ ,  $R_{icc}$  represent the cables connecting the transformer to the busbar.

Table 3 shows the parameters of the RMU model obtained averaging the values coming from tests at six RMUs in a frequency range from 200 kHz up to 5 MHz. In Table 3,  $l_{c1}$  and  $l_{c2}$  and  $u_1$  and  $u_2$  are the respective length and propagation speed of the XLPE and PILC cable. The chosen frequency range is the most relevant for the propagation of PD signals in MV cables with a length from hundreds of

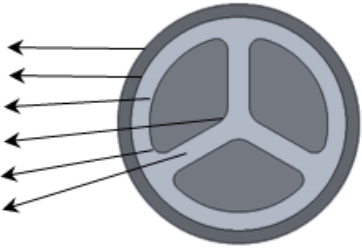


**Fig. 6** Current (blue) and voltage (red) response upon a delta-function like PD; amplitude spectrum (left) and unwrapped phase angle (right) for a PD at 65 m from the right end of the XLPE cable.

**Table 1** XLPE cable characteristics

Cable parameters	Value		
Al conductors, $r_1$	8.55 mm		
conductor screen, $r_2$	9.35 mm		
XLPE insulation, $r_3$	12.75 mm		
insulation screens, $r_4$	14.00 mm		
conductors-centre, $d_k$	16.16 mm		
filler material, $r_{p1}$	30.15 mm		
swelling tape, $r_{p2}$	30.50 mm		
Cu earth screen, $r_{p3}$	31.50 mm		
PVC jacket, $r_{p4}$	33.00 mm		
conductivity conductor (Al), $\sigma_{Al}$	$3.69 \cdot 10^7$ S/m		conductor/insulation screen: $\epsilon_r=1000$ , $\sigma=33$ S/m
conductivity earth screen (Cu), $\sigma_{Cu}$	$5.84 \cdot 10^7$ S/m		swelling tape: $\epsilon_r=1000$ , $\sigma=100$ S/m
relative permittivity XLPE, $\epsilon_{r,xlpe}$	2.26-0.001j		conductivities XLPE and filler material are 0 S/m
relative permittivity filler, $\epsilon_{r,filler}$	4.0		

**Table 2** PILC cable characteristics

Cable parameters	Value	
outer radius earth screen	32.5 mm	
inner radius earth screen	29.0 mm	
radius conductors	24.0 mm	
inner rounding radius conductors outer	5.0 mm	
rounding radii conductors	3.0 mm	
distance between conductors	5.9 mm	
conductivity conductor (Al), $\sigma_{Al}$	$3.69 \cdot 10^7$ S/m	
conductivity earth screen (Pb), $\sigma_{Pb}$	$4.70 \cdot 10^6$ S/m	
relative permittivity PILC, $\epsilon_{r,pilc}$	3.5-0.1j	
conductivity PILC, $\sigma_{PILC}$	0 S/m	

**Table 3** Fitted parameters used for modelling the high-frequency behaviour of an RMU [13]

$Z_{c1}$ ( $\Omega$ ) <sup>1</sup>	$Z_{c2}$ ( $\Omega$ ) <sup>1</sup>	$l_{c1}$ (m) <sup>1</sup>	$l_{c2}$ (m) <sup>1</sup>	$u_1$ (m/s) <sup>1</sup>	$u_2$ (m/s)	$L_c$ ( $\mu$ H)	$L_{bb}$ ( $\mu$ H)	$C_{tr}$ (nF)	$L_{tr}$ ( $\mu$ H)	$R_{tr}$ ( $\Omega$ )	$C_{tcc}$ (nF) <sup>3</sup>	$L_{tcc}$ ( $\mu$ H)	$R_{tcc}$ ( $\Omega$ )
7.9	6.6	425	75	$1.036 \cdot 10^8$	$1.580 \cdot 10^8$	0.34	0.12	2.5	2.6	12	1.9	1.2	8.6

- 1) Characteristic impedances  $Z_{c1}$  and  $Z_{c2}$  and propagation speeds  $u_1$  and  $u_2$ , obtained from electromagnetic modelling of the cable design for XLPE and PILC respectively (three phases with respect to earth screen)
- 2) The capacitance  $C_{tcc}$  is determined from the cable length (up to 10m) and its specifications

metres up to several kilometres as shown in [9] and [13]. If the cable to be diagnosed is connected in compartment 1, it is loaded through  $L_c$  and  $L_{bb}$  to the branches representing the cable in compartment 2 and to the parallel branches of the transformer and its connection in compartment 3.

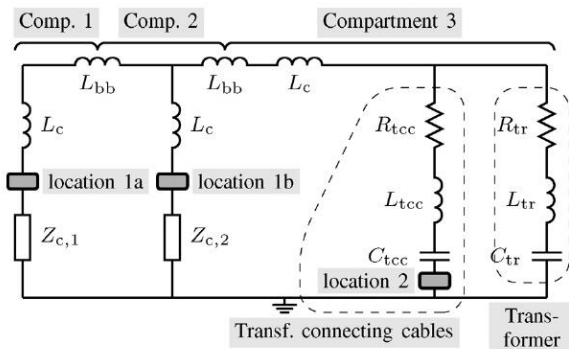


**Fig. 7** RMU compartment model [13].

Figure 8 shows the impedance of the RMU, seen from the diagnosed cable, with a second connected cable being either an XLPE or a PILC cable. There are resonances in the

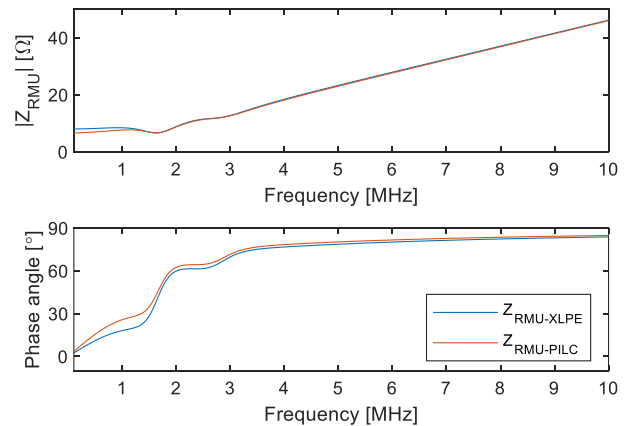


**Fig. 8** Impedance of an RMU with a distribution transformer and a second connected cable (XLPE or PILC).



low megahertz range caused by the inductances, from the loops formed by the busbar connection, and the capacitances, from the transformer and connecting cables. These resonances, which occur at relevant frequencies for PD signal propagation along the cables, may distort the PD signal waveform. At lower frequencies the impedance of the second

connected cable (the PILC cable) dominates the impedance and beyond the resonances, the substation impedance increases due to the inductances.

The adopted RMU model was defined for a frequency range up to about 5 MHz [13]. The modelling of connection details inside RMUs, specific to each RMU, becomes

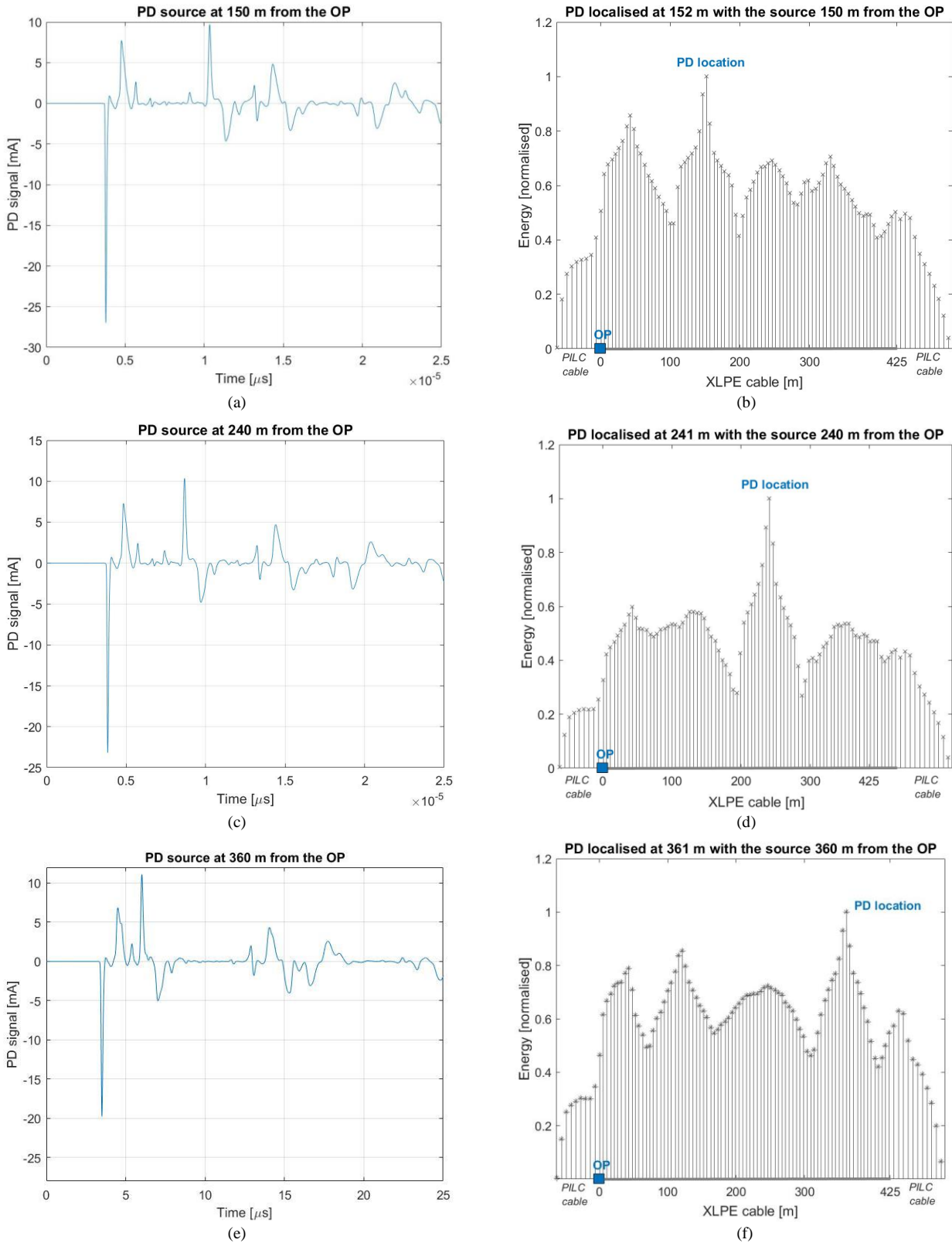


**Fig. 9** PD signals recorded (simulated) at the OP (on the left) and the EMTR localisation of the PD source in the monitored XLPE cables section (on the right) when the PD source is 150 m, 240 m and 360 m away from the OP.

important at frequencies beyond 5 MHz. But these higher frequencies hardly contribute due to PD signal attenuation. Therefore, to the aim of power cable diagnostics, the adopted RMU model provides a representative behaviour of the influence of RMUs on PD waveforms.

#### 4. Numerical results and analysis

To test the performance of the EMTR method to localise a PD source in the XLPE cable section of the system under study, a lossless 1D TLM model of the whole system shown in Figure 3 has been developed to perform the time reversal simulations. This distinction is important because it is intended to demonstrate how well a generic model can be used to localise the PD event and show that an exact facsimile of the network under consideration is not necessary.

The direct time (DT) simulation, during which a PD event is simulated in a point of the system and the PD signals, propagating along the lines, are recorded at the OP, is performed using the lossy model of the system under study (RMU and lines) described in the previous Section 3.

Considering the electromagnetic modelling of the cables reported in tables 1 and 2 and in Figure 4, in the 1D TLM model the used characteristic impedances of the XLPE and PILC cables and propagation speeds have been evaluated at a frequency of 1 MHz. The characteristic impedances and propagation velocities are close to constant around this frequency. It is also in the range of relevant signal frequencies for detecting PD signals in power cables [13]. The values are  $Z_{XLPE} = 7.9 \Omega$  and  $u_{XLPE} = 1.036 \cdot 10^8$  m/s,  $Z_{PILC} = 6.6 \Omega$ , and  $u_{PILC} = 1.580 \cdot 10^8$  m/s, respectively for the XLPE cable and PILC cable, as reported in Table 3.

The RMU was modelled with a 3-m long TLM model and with a characteristic impedance,  $Z_{RMU}$ , chosen equal to  $Z_{RMU} = 10 \Omega$ , i.e., higher than the characteristic impedances of both of the cables connected to it. This is to obtain a relative reflection coefficient  $\Gamma_{RMU} > 0$  because the RMU only causes a distortion mainly for high frequencies and is hardly visible when the wavelengths associated with the remaining frequencies after signal attenuation exceed the RMU size, as explained in [9].

To perform the analysis, the PD signal was collected at the observation point (OP), located at the right end of the RMU, in Figure 3, where the XLPE cable under test is connected. Then, the collected PD signal was time reversed and injected into the 1D TLM model and several time reversal simulations were performed. For each PD signal measurement, an initial record length corresponding to a time equal to  $3 \mu\text{s}$  was considered.

In Figure 9 the simulation results of the EMTR-based method are shown when the PD source is located, respectively, at a distance of 150 m, 240 m and 360 m from the OP. In Figure 9, the simulated PD current signals recorded at the OP during the DT simulation in the analysed cases are also reported. Considering the plots (a), (c), (e) in Figure 9, the interpretation of the individual peaks can become hard since the waveform is affected by several reflections from the relatively short PILC cables. Also, the RMU further disguises individual peak structures. The worst case corresponds to the PD source near the far end of the XLPE cable, i.e., 360 m away from the OP and 65 m from the right end of the XLPE cable. In this case, the reflection coming from the PILC cable on its right coincide with the direct PD signal.

For the localisation procedure, a discretization step of 5 m was chosen between two consecutive positions of the GPDs moved along the system during the time reversal simulation. This was to provide trade-off between reasonable resolution and speed of calculation. As Figure 9 shows, the method is able to localise the PD source with a relative error, with respect to the XLPE cable length, of less than 0.1%. Despite the distortion of the PD signal due to the frequency dependence of the system impedances and the reflections coming from the impedance mismatches of the line and the other cable section connected to the RMU, the EMTR-based method is able to localise the source with excellent accuracy.

A total computational time of a few seconds is necessary for localising the PD source, using a 64-bit pc with an Intel® Core™ i7-8700K, CPU at 3.70 GHz, 32 GB RAM and a 1 TB disk. In this case, a time window equal to  $2.5 \mu\text{s}$  was chosen for the PD signal measurement. Such window is large enough to measure the direct PD signal from the source and the reflections from the other cables considering the propagation speeds for the two cable types. A longer measurement time window would only increase the computational time of the time reversal simulation without improving the already satisfactory results.

#### 5. Conclusion

The question being addressed in this paper was whether EMTR could detect PD events in representative mains configurations, and if so, how well. The performance of the EMTR-based method to localise PDs in the presence of interfering PD reflected signals coming from the impedance discontinuities of the circuit and by the reflections from the cable ends of the PILC cables connected to the RMU was analysed. A description of the EMTR PD localisation method was given and the models used to simulate the grid components, RMU and power cables, useful to reproduce the PD signal distortion were described.

The results showed that the method is able to localise the PD source in the analyzed configuration with a relative error, with respect to the length of the monitored line section, of less than the 0.1 %. The results also showed that the EMTR-based method can localise the PD source using a PD signal measured at a monitoring point located at an RMU somewhere along the line and not necessarily at the line termination.

#### 6. References

- [1] F. Auzanneau, "Wire Troubleshooting and diagnosis: Review and perspectives", Progress in Electromagnetics Research B, Vol. 49, 2013.
- [2] M. S. Mashikian, R. Bansal, R. B. Northrop – "Location and Characterization of Partial Discharge sites in Shielded Power cables" - *IEEE Trans. on Pow. Del.*, Vol. 5, Issue 2, April 1990.
- [3] G. Robles, M. Shafiq, J. M. Martínez-Tarifa, "Multiple Partial Discharge Source Localization in Power Cables Through Power Spectral Separation and Time-Domain Reflectometry", *IEEE Trans, on Instrumentation and Measurement*, Vol. 68, Issue 12, Dec. 2019.
- [4] C. C. Yii, M. N. K. H. Rohani, M. Isa, and S. I. S. Hassan, "Multi-end PD location algorithm using segmented correlation and trimmed mean data filtering techniques for

MV underground cable,” IEEE Trans. on Dielectrics and Electrical Insulation, vol. 24, Issue 1, Feb. 2017.

[5] F. P. Mohamed, W. H. Siew, J. J. Soraghan, S. M. Strachan, “Partial discharge location in power cables using a double ended method based on time triggering with GPS”, IEEE Transactions on Dielectrics and Electrical Insulation, Vol. 20, Issue 6; Dec 2013.

[6] P. Wagenaars, P. A. A. F. Wouters, P. C. J. M. van der Wielen, E. F. Steennis, “Influence of ring main units and substations on online partial-discharge detection and location in medium-voltage networks,” IEEE Trans. Power Delivery, vol. 26, Issue 2, Apr. 2011.

[7] A. Ragusa, H. Sasse, A. Duffy, F. Rachidi, M. Rubinstein, “Electromagnetic time reversal method to locate partial discharges in power networks using 1D TLM modelling”, IEEE L-EMCPA, Vol.3, Issue1, March 2021.

[8] A. Ragusa, H. Sasse, A. Duffy, F. Rachidi, M. Rubinstein – “Application to real power networks of a method to locate partial discharges based on electromagnetic time reversal”, IEEE Trans. on Power Delivery, Vol, 37, Issue 4, August 2022.

[9] A. Ragusa, P. A. A. F. Wouters, H. Sasse, A. Duffy, “The effect of the ring mains units for on-line partial discharge location with time reversal in medium voltage networks”, IEEE Access, March 2022.

[10] F. Rachidi, M. Rubinstein, M. Paolone, Electromagnetic Time Reversal – Application to Electromagnetic Compatibility and Power System - John Wiley & Sons Ltd, 2017; pp. 95-97.

[11] A. Ragusa, P. A. A. F. Wouters, H. Sasse, A. Duffy, F. Rachidi, M. Rubinstein, “Electromagnetic time reversal applied to online partial discharge location in power cables: influence of interfering reflections from the cable circuit”, 11th Inter. Conference on Computation in Electromagnetics, 11-14 April 2023, Cannes, France.

[12] C. Christopoulos, The transmission-line modeling method – TLM, Wiley-IEEE Press, 1995.

[13] P. Wagenaars, P. A. A. F. Wouters, P. C. J. M. van der Wielen, E. F. Steennis, “Influence of ring main units and substations on online partial-discharge detection and location in medium-voltage networks,” IEEE Trans. Power Delivery, vol. 26, Issue 2, pp. 1064-1071, Apr. 2011.